Angle-resolved ultraviolet photoelectron spectroscopic study of Si(001)-(2×1)/K and Si(001)-(2×1)/Cs surfaces

Y. Enta, T. Kinoshita, S. Suzuki, and S. Kono
Department of Physics, Faculty of Science, Tohoku University, Sendai, Miyagi 980, Japan
(Received 12 April 1988)

Angle-resolved ultraviolet-photoelectron-spectroscopy (ARUPS) spectra of the Si(001)-(2×1)/K and Si(001)-(2×1)/Cs surfaces have been measured for alkali-metal-atom coverages ranging from zero to saturation. Valence-band spectra and corresponding binding energy versus wave vector diagrams for the full-coverage Si(001)-(2×1)/K and Si(001)-(2×1)/Cs surfaces show that the two surfaces are semiconducting, in contrast to a generally accepted view of the one-dimensional and metallic alkali chain of the alkali/Si(001) systems. Plausible dispersions of surface-state bands are proposed for the full-coverage Si(001)-(2×1)/K and Si(001)-(2×1)/Cs surfaces. Normal-emission ARUPS spectra of outermost core levels of K and Cs have been found to be essentially invariant with alkali-metal-atom coverage in spite of large changes in work function. The effect of substrate doping on the ARUPS spectra has been examined.

I. INTRODUCTION

Study of alkali-metal adsorption on semiconductor surfaces is the basis for understanding, for example, negative electron affinity (NEA) and alkali-assisted catalytic reactions on semiconductor surfaces. K or Cs adsorbed on a Si(001) surface is a prototypical adsorption system to which many modern techniques of surface science have been applied. Holtom and Gundry[1] made a pioneering work on a Cs/Si(001)-(2×1) system using low-energy electron diffraction (LEED), Auger-electron spectra (AES), and other techniques. They showed that the surface order of Si(001)-(2×1) is basically invariant under the adsorption of Cs. It was postulated from this fact that a one-dimensional chain of Cs atoms is formed on the Si(001)-(2×1) surface. This postulation of one-dimensional alkali chain (1D AC) became a basic assumption in the following interpretation of Si(001)-(2×1)/K surface.

Aruga *et al.*[2] measured angle-resolved electron-energy-loss spectra of a full-coverage Si(001)-(2×1)/K surface. Electronic structures of the Si(001)-(2×1)/K surface were analyzed theoretically based on the 1D AC model.[3,4] Although the two theoretical analyses are not in agreement with each other as to the nature of the K-substrate bonding, both found the surface-state bands to be metallic. Less quantitative works[5,6] have been reported on the Cs/Si(001) system since the work of Holtom and Gundry.[1] Interpretation of the two works was also based on the 1D AC.

In a previous paper,[7] we reported angle-resolved ultraviolet-photoelectron-spectroscopy (ARUPS) study of the K/Si(001) system. Contrary to the expectation from the 1D AC, our ARUPS spectra showed semiconducting nature of the Si(001)-(2×1)/K surface. In an inverse photoemission study, Batra *et al.*[8] reported a dispersion of unoccupied surface states of the Si(001)-(2×1)/K surface. The result was also not in agreement with the expectation from the 1D AC model. There is a large difference between the metallic 1D AC surface and the observed semiconductive Si(001)-(2×1)/K surface. For the metallic surface, the coverage of K is assumed to be $\frac{1}{2}$ML [1 monolayer (ML) being the surface atomic density of a truncated Si(001)-(1×1) surface; $6.8\times10^{14}/\text{cm}^2$]. With this coverage, the semiconductive Si(001)-(2×1)/K surface would not result unless the charge neutrality at the surface were broken.[7] In a subsequent study, we have observed that the Si(001)-(2×1)/Cs surface is also semiconducting. We describe in this paper a full account of ARUPS works on both the K/Si(001) and Cs/Si(001) systems.

II. EXPERIMENT

Experiments were performed with a UHV photoelectron spectrometer which basically consists of a hemispherical electron analyzer, a He resonance lamp, a cylindrical-mirror-type Auger analyzer, and LEED optics.[7] The base pressure of the chamber was $\sim5\times10^{-11}$ Torr and the energy and angle resolutions of the spectrometer were ~0.1 eV and $\sim\pm1.5°$, respectively. Two types of Si(001) wafer were used. One is *p* type, 20–40 Ω cm, $0.5\times4\times25$ mm^3 and the other is *n* type, 8–18 mΩ cm, $0.28\times4\times25$ mm^3. For simplicity, the former is called a nearly intrinsic sample and the later a high-dope *n*-type sample in this paper. Both types of Si wafer were pretreated[7] and cleaned *in situ* by cycles of Ar ion bombardment followed by annealing at ~900 °C. After cleaning, no contaminants were observed in the AES spectra, and LEED showed clear two-domain 2×1 patterns. K and Cs were deposited onto a room-temperature substrate from chromate dispensers (SAES getter) under a pressure of $4-6\times10^{-10}$ Torr. K- and Cs-adsorbed samples for the ARUPS experiments were prepared every 1 and 4 h of ARUPS measurements, respectively. Cleaning of the K/Si(001) and Cs/Si(001) surfaces was carried out

by annealing at ~900 °C for 30 sec combined with occasional Ar^+ bombardment (typically once a day). The annealing of the sample was carried out by passing direct current through the sample wafer and temperature was monitored by an infrared and an optical pyrometer. Work functions of the clean and alkali-adsorbed samples were measured from low-energy cutoff of normal-emission UPS spectra observed with a sample bias voltage of 10 V.

III. EXPERIMENTAL RESULTS

A. Si(001)-(2×1)/K surface

Figure 1 shows changes in work function and Auger electron intensity ratio $I(\mathrm{K}(LMM))/I(\mathrm{Si}(LMM))$ as a function of the duration of K deposition. The Auger intensity ratio increases almost linearly up to ~4 min and stays constant afterward. This proves that the uptake of K on the Si(001) surface is at a roughly constant rate until saturation takes place. The effect of variation in the reference Si Auger intensity is estimated to change the linearity very little. The work function decreases very drastically and almost linearly at the early stage of the K deposition. The decrease in work functions saturates after around 4 min. On continued deposition there is only a very small work function increase (cf. Fig. 3). LEED patterns observed were two-domain 2×1 patterns throughout the experiment in Fig. 1 except for an additional but weak two-domain 3×2 patterns for $\Delta\Phi \sim -1.9$ eV.

Figure 2 shows normal-emission ARUPS spectra of the Si(001)-(2×1)/K surface as a function of the change in work function $\Delta\Phi$ which corresponds to $\Delta\Phi$ in Fig. 1. For $-1.1\ \mathrm{eV} \lesssim \Delta\Phi$, a peak at the Fermi level E_F which is characteristic of a metallic sample is dominant; it shows a

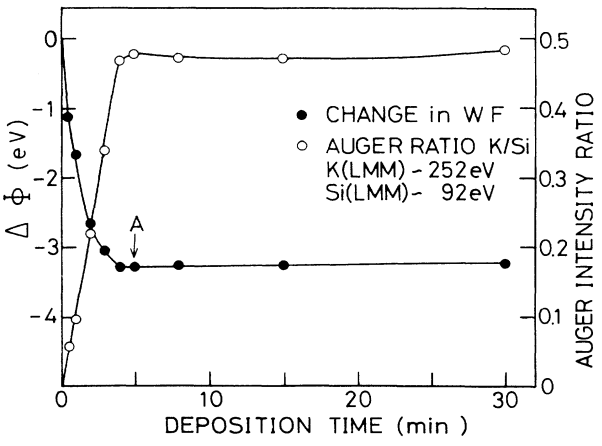

FIG. 1. Changes in work function and Auger electron intensity ratio for the K/Si(001) system as a function of the duration of K deposition. The substrate is at room temperature during the K deposition. Work function for the clean Si(001)-(2×1) was ~4.8 eV, and the substrate was a nearly intrinsic wafer.

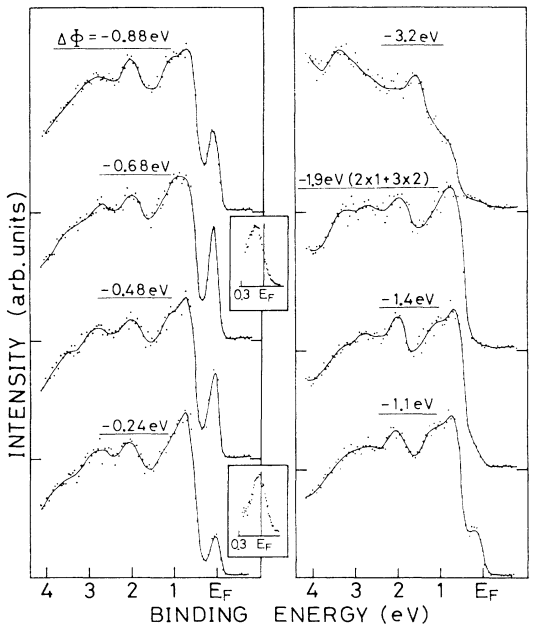

FIG. 2. Normal-emission ARUPS spectra (He I) for the various stages of K adsorption on the Si(001) surface. Incident light is at 45° along ⟨110⟩ azimuth. The $\Delta\Phi$'s are the measures of the degree of K adsorption (cf. Fig. 1). The insets are the expanded spectra near the E_F for $\Delta\Phi = -0.24$ and -0.68 eV. The substrate was the same as in Fig. 1.

maximum intensity around $\Delta\Phi \sim -0.7$ eV. For the clean Si(001)-(2×1) surface, a similar but weak metallic peak is found and is attributed to dangling bond states of Si dimers in area of disordered asymmetric dimers.[9] Another important finding in Fig. 2 is that in spite of the drastic change in the metallic peak, other spectral features for binding energies $E_b \gtrsim 0.5$ eV are nearly invariant up to $\Delta\Phi = -1.9$ eV.

From $\Delta\Phi = -1.9$ eV to -3.2 eV, the whole spectrum changes. To see this change closer, we show detailed spectra for $-2.59 \gtrsim \Delta\Phi \gtrsim -3.21$ eV in Fig. 3. Figure 3(a) is normal-emission valence-band spectra as in Fig. 2. There occurs an essential spectral change between $\Delta\Phi = -2.59$ and -2.99 eV before reaching the minimum in Φ. After $\Delta\Phi = -2.99$ eV, the spectra do not change essentially except that the whole spectra tend to shift to the higher binding energy side as a small peak at the E_F develops. The small metallic peak at the E_F starts to develop just after Φ reaches the minimum, namely for the deposion time larger than ~5.0 min in Fig. 1. The Auger ratio curve in Fig. 1 shows that the amount of adsorbed K has essentially reached a saturation value just before the $\Phi_{\min}$ and that even after the $\Phi_{\min}$, the K coverage does not appear to change within an experimental error. If there were an essential difference in the surface properties between the semiconducting Si(001)-(2×1)/K surface just before the $\Phi_{\min}$ and the Si(001)-(2×1)/K surface after the $\Phi_{\min}$, there would be appreciable differences in the K coverage and the spec-

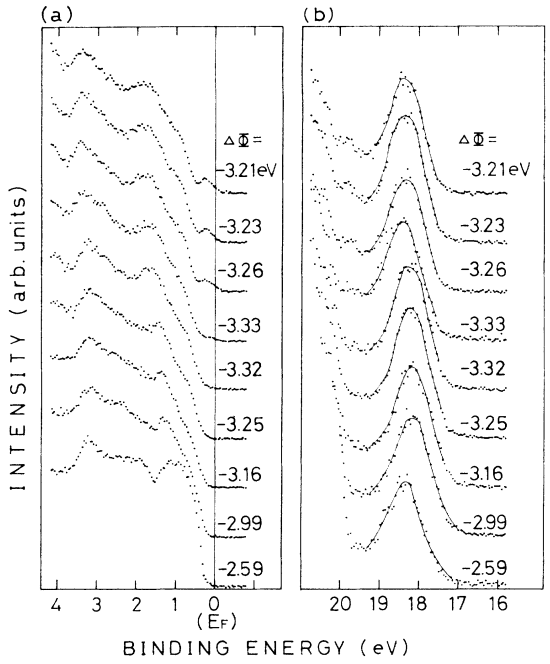

FIG. 3. (a) Normal-emission ARUPS spectra of the valence band (He I) and (b) K $3p$ levels (He II) for the Si(001)-(2×1)/K surface as a function of $\Delta\Phi$. The $\Delta\Phi$ corresponds to the K deposition time of ~3 to 30 min in Fig. 1. Spin-orbit splitting of K $3p$ levels is not resolved. The substrate was the same as Fig. 1.

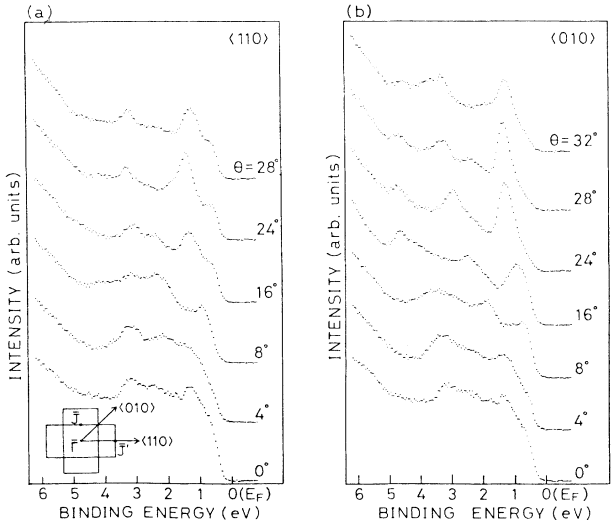

FIG. 4. Representative ARUPS spectra (He I) of the Si(001)-(2×1)/K surface at K-adsorption stage just before reaching the Φ_{min} ($\Delta\Phi=-3.15$ eV) in Fig. 3. θ is the polar angle of photoelectron detection, and it is changed along (a) ⟨110⟩ and (b) ⟨010⟩ directions. Inset shows relation to two-domain 2×1 surface Brillouin zone. The sample was a high-dope n-type wafer, but no difference was found for a nearly intrinsic wafer.

tral profile between the two surfaces. Therefore, a full-coverage semiconducting Si(001)-(2×1)/K surface is essentially formed just before Φ reaches the minimum and that, upon further K deposition, a metallic peak, which may be due to the small amount of excess K metal, starts to pin the Fermi level at the surface and shift the whole spectrum. This hypothesis is justified when we compare E_b-$k_{\parallel}$ (binding energy versus wave vector) diagrams for the samples at $\Delta\Phi\sim-3.15$ eV (just before Φ minimum) and $\Delta\Phi\sim-3.2$ eV (saturation) in Figs. 4 and 5.

Figure 3(b) shows normal-emission ARUPS spectra of K $3p$ levels as excited by He II ($h\nu=40.8$ eV) for the same conditions in Fig. 3(a). The spectra look about the same

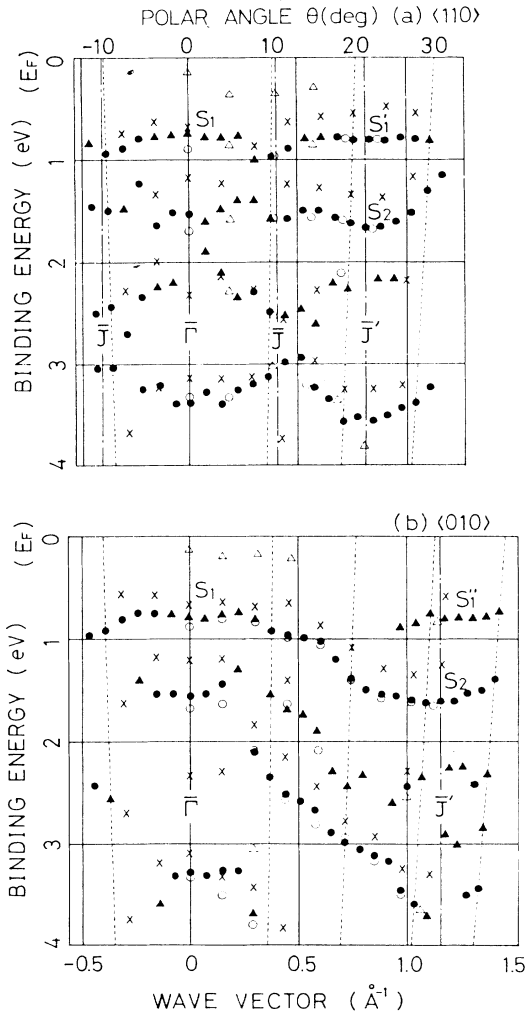

FIG. 5. E_b-$k_{\parallel}$ diagrams for the Si(001)-(2×1)/K surfaces with different degrees of K adsorption and substrate doping (a) along ⟨110⟩ direction and (b) along ⟨010⟩ direction. Solid symbols are from the previous result (Ref. 7) for a nearly intrinsic wafer with K-adsorption stage just after the Φ_{min}. Crosses are for a high-dope n-type wafer with K-adsorption stage just before the Φ_{min}. Open symbols are for a high-dope n-type with K-adsorption stage of saturation coverage.

for all the conditions; the energy position of K $3p$ levels changes slightly to the low-binding-energy side between $\Delta\Phi=-2.59$ and -2.99 eV corresponding to the change in valence-band spectra. A slight shift of K $3p$ peak after Φ_{min} must be related to the change in E_F pinning position in Fig. 3(a).

In the previous study,[7] we showed ARUPS spectra and E_b-$k_\parallel$ diagrams of a sample for $\Delta\Phi\approx-3.26$ eV which corresponds to K-adsorption stage just after the Φ_{min}. The substrate was the nearly intrinsic sample. For the present study, we show in Figs. 4 and 5 ARUPS spectra and E_b-$k_\parallel$ diagrams, respectively, of the high-dope n-type sample for $\Delta\Phi\approx-3.15$ eV which corresponds to K-adsorption stage just before the Φ_{min}. The spectra in Fig. 4 are obviously very similar to those in Fig. 2 of the previous report.[7] Very weak structure near the E_F found in the previous spectra is absent for all the θ, thus the semiconducting nature of the Si(001)-(2×1)/K surface is very clear. When we examine the spectra very closely, we notice that the spectral features are shifted by 0.2–0.3 eV to the lower-binding-energy side in Fig. 4 as compared to those in Fig. 2 of Ref. 7.

This solid shift becomes obvious when E_b-$k_\parallel$ diagrams are compared in Fig. 5. The solid symbols are from the previous result[7] and the crosses are from the results in Fig. 4. The two E_b-$k_\parallel$ diagrams are shifted by $\sim$0.2–0.3 eV from each other except for weak or broad structures for which the peak positions are somewhat ambiguously determined. In Fig. 5 we also show E_b-$k_\parallel$ diagrams (open symbols) for the n-type high-dope sample for $\Delta\Phi\approx-3.30$ eV, which corresponds to the K-adsorption stage just after the Φ_{min}. The E_b-$k_\parallel$ diagrams for this sample show almost exactly the same dispersion as those for the previous sample[7] except for a noticeable additional structure near the E_F. Therefore, the E_b-$k_\parallel$ diagrams for the three kinds of surface appeared to be essentially the same. The solid shift of the spectra appeared to be related to the E_F pinning by a metallic state possibly due to excess K atoms, and the metallic peak is higher for the high-dope n-type sample than for the nearly intrinsic sample. When the Si(001)-(2×1)/K surface is not Fermi-level pinned by the metallic state, the Si(001)-(2×1)/K surface appears very semiconducting as evidently seen in Fig. 4. Therefore the assumption of the metallic 1D AC Si(001)-(2×1)/K surface is denied.

Two obvious surface-related bands are seen in Fig. 5, i.e., S_1 and S_2 bands. The S_1' band must be the same band as S_1 since we have two-domain 2×1 surface and corresponding surface Brillouin zones are overlapped along the ⟨110⟩ direction. The S_1'' band may have the same origin as the S_1 band, and it may be related to disordered and/or domain-boundary regions of the surface. It is also of importance to note that no effect of doping level is found for the semiconducting Si(001)-(2×1)/K surface at the K-adsorption stage just before the Φ_{min}.

B. Si(001)-(2×1)/Cs surface

Figure 6 shows changes in work function and Auger intensity ratios I(Cs(*MNN*))/I(Si(*LMM*)), I(Cs(*NOO*))/I(Si(*LMM*)) as a function of the duration of deposition. The Auger ratios increase almost linearly up to $\sim$9 min and stay constant afterward. This proves that the uptake of Cs on the Si(001) surface is at a constant rate before it saturates. The effect of a change in the reference Si(*LMM*) Auger intensity is estimated to be very small. The work function shows a distinct minimum at $\sim$5 min for the Cs/Si(001) system, which was not the case for the K/Si(001) system. LEED patterns observed were two-domain 2×1 patterns throughout except for additional but weak two-domain 3×2 patterns for $\Delta\Phi=-2.3\sim-2.8$ eV.

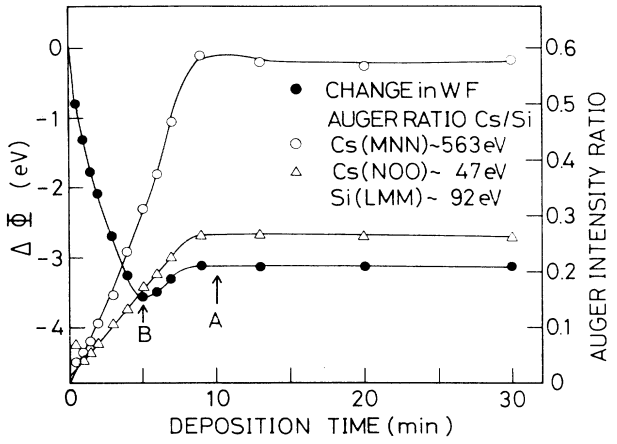

FIG. 6. Changes in work function and Auger electron intensity ratios for the Cs/Si(001) system as a function of the duration of Cs deposition. The substrate was a high-dope n-type wafer and kept at room temperature during Cs deposition.

Figure 7 shows normal-emission ARUPS spectra of the Si(001)-(2×1)/Cs surfaces for the early stages of Cs deposition, $-1.79\lesssim\Delta\Phi\lesssim0$ eV. For the Cs/Si(001) system, the structure at the E_F has rather strong intensity as compared to that for the K/Si(001) system shown in Fig. 2. This structure at the E_F changes its position to the higher-binding-energy side with increase in Cs deposition. This structure finally disappears for $\Delta\Phi\lesssim-2$ eV (cf. Fig. 8). The rest of the spectral profiles shows a gradual change with decrease in work function in Fig. 7. Figure 8 shows normal-emission ARUPS spectra for the whole range of $\Delta\Phi$. The spectra for $\Delta\Phi\lesssim-3.24$ eV have less structures with a gradual change with $\Delta\Phi$. For $-3.30\lesssim\Delta\Phi\lesssim-3.11$ eV, we notice a slight increase of intensity at the E_F. For these $\Delta\Phi$'s, the Cs uptake is nearly saturated. Therefore, the small peak at the E_F is likely due to a small amount of excess Cs metal on the Si(001)-(2×1)/Cs surface for the same reason as explained for the Si(001)-(2×1)/K surface.

We have observed and compared detailed ARUPS spectra for the sample at Φ_{min} ($\Delta\Phi=-3.57$ eV, B point in Fig. 6) with ARUPS spectra at Cs saturation (A point in Fig. 6). It appeared that although gross features were alike for the two samples, the spectra at Cs saturation were rich in fine structures. This indicates that the Si(001)-(2×1)/Cs surface at Φ_{min} is not a different surface

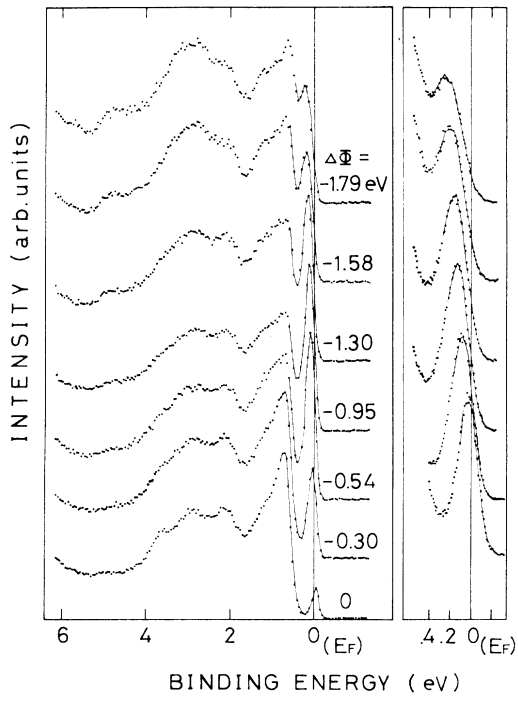

FIG. 7. Normal-emission ARUPS spectra (He I) for the early stage of Cs adsorption on the Si(001)-(2×1) surface. The ΔΦ's are the measures of the degree of Cs adsorption (cf. Fig. 6). The spectra on the right are the detailed spectra near the E_F. Other conditions are the same as in Fig. 6.

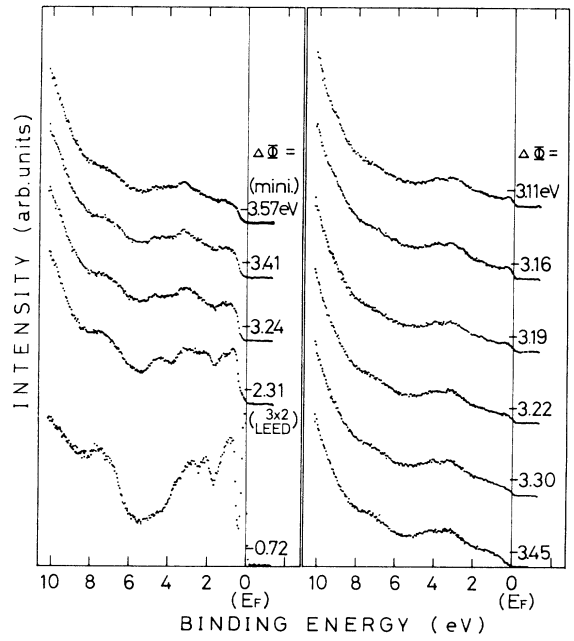

FIG. 8. Normal-emission ARUPS spectra (He I) for the whole range of Cs deposition on the Si(001)-(2×1) surface. Conditions are the same as in Figs. 6 and 7.

from the Si(001)-(2×1)/Cs surface at Cs saturation, but it is in the middle of growth of the Si(001)-(2×1)/Cs surface to Cs saturation.

Figure 9 shows normal-emission ARUPS spectra of Cs 5*p* levels as a function of ΔΦ. There is no essential change in the spectra as to the peak position and width for $-3.57 \lesssim \Delta\Phi \lesssim -0.72$ eV. For $\Delta\Phi \gtrsim -3.3$ eV after passing the Φ_{min}, the spectral width of the two spin-orbit components become larger, and for $\Delta\Phi = -3.11$ eV there may exist two components in each of the spin-orbit components.

Figure 10 shows ARUPS spectra of the near-saturation Si(001)-(2×1)/Cs surface at the *A* point in Fig. 6 which must be close to the spectra of an intrinsic Si(001)-(2×1)/Cs surface. The spectrum at $\theta = 0°$ shows a small peak just below the E_F. The small peak is likely due to excess Cs metal as explained for Fig. 8. This can be justified by the facts that the E_F level cuts at the foot of the small peak and that the small peak is close to the E_F only near the $\bar{\Gamma}$ point. Therefore, the intrinsic Si(001)-(2×1)/Cs surface is unlikely to be metallic. This can be further confirmed in E_b-$k_{\parallel}$ diagrams in Fig. 11. They are compared with the results for the Si(001)-(2×1)/K surface. Surface-related bands for the Si(001)-(2×1)/Cs surface are marked as S_1, S_1', S_1'', S_2, and S_3; the S_1' band must be identical to the S_1 band, and the S_1'' band may also be the case as explained for the Si(001)-(2×1)/K surface. It appears that the S_1 band for the Si(001)-

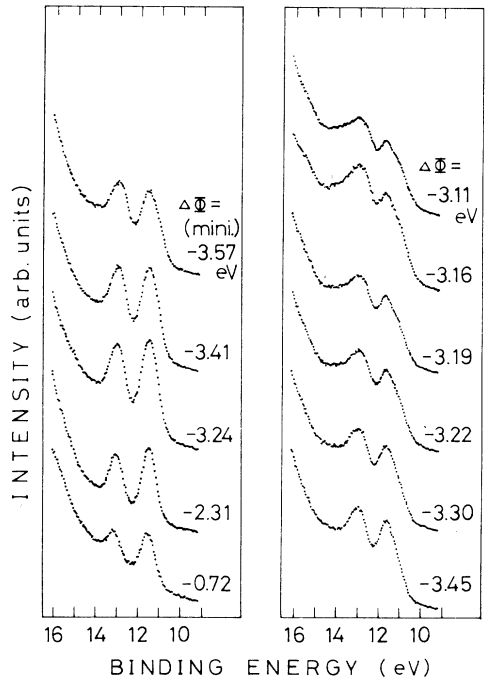

FIG. 9. Normal-emission ARUPS spectra of Cs 5*p* levels (He I) for the Si(001)-(2×1)/Cs surface as a function of ΔΦ (cf. Fig. 6). The spectra were measured with a bias voltage of 5 V on the sample for clarity of the spectra. Other conditions are the same as in Figs. 6–8.

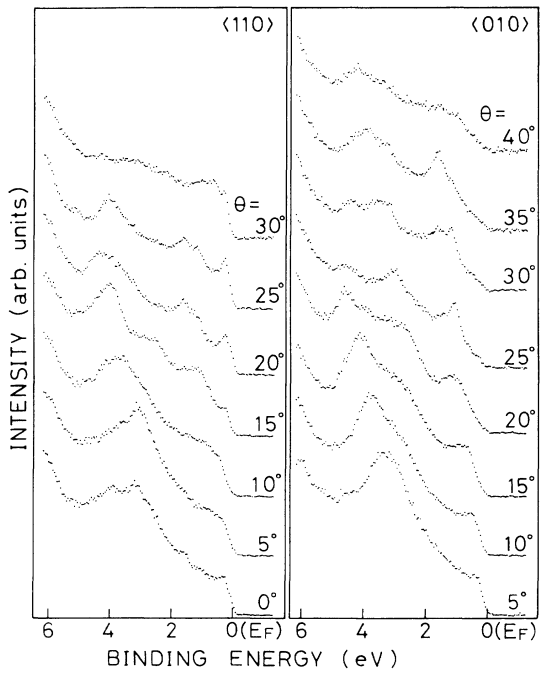

FIG. 10. Representative ARUPS spectra (He I) of the Si(001)-(2×1)/Cs surface as a function of electron polar angle θ at Cs-adsorption stage of A point in Fig. 6. The substrate was a nearly intrinsic wafer and other conditions are the same as in Figs. 6–8.

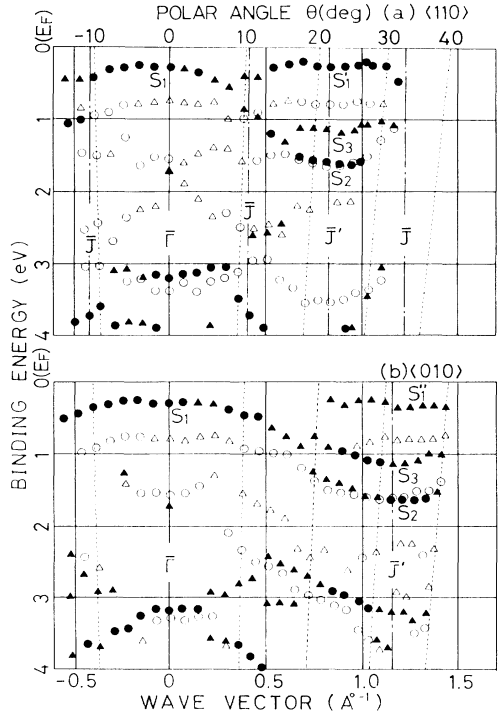

FIG. 11. E_b-$k_{\parallel}$ diagrams (solid symbols) for the Si(001)-(2×1)/Cs surface, (a) along ⟨110⟩ and (b) ⟨010⟩ directions. Open symbols are for the Si(001)-(2×1)/K surface taken from those of solid symbols in Fig. 5.

(2×1)/Cs surface shifts to lower-binding-energy side as compared to the Si(001)-(2×1)/K surface and that the S_2 band for the Si(001)-(2×1)/K surface splits to S_2 and S_3 bands for the Si(001)-(2×1)/Cs surface.

IV. DISCUSSION

A. Changes in Auger intensity and work function

As seen in Figs. 1 and 6, both K and Cs Auger intensity ratios increase almost linearly up to certain values. The ratios are referenced to Auger intensity of the substrate Si. Even if we take into account an exponential decay of the Si Auger intensity, the linear nature of the Auger intensities of alkali-adatoms is not changed very much. Therefore, K and Cs adsorptions take place up to saturation at almost constant sticking probabilities onto the room-temperature Si(001)-(2×1) substrate. K and Cs adsorptions essentially stop at certain coverages.

Oellig and Miranda[10] reported Auger work on a K/Si(001) system at 300 K. They claimed that the K adsorption takes place in a layer-by-layer mode which contradicts with our finding. It may be possible that actual substrate temperatures may differ in the two cases. Ortega *et al.*[11] reported Auger intensity changes for a Cs/Si(001) system at substrate temperatures of 200 and 300 K, which is in qualitative agreement with ours.

Work-function changes for K/Si(001) and Cs/Si(001) systems have been reported by several workers. They are compared in Table I. For K/Si(001), the $\Delta\Phi_{sat}$ values of Refs. 10 and 12 are very different from ours, which may be due to difference in actual experimental conditions. For Cs/Si(001), all the values are in reasonable agreement. The work-function changes are further discussed in relation to the core-level spectra of alkali atoms.

B. Changes of the Si(001)-(2×1) surface during early stage of K and Cs adsorptions

At the early stage of K and Cs adsorptions, a dramatic variation of intensity of a metallic peak is found in Figs. 2 and 7. The metallic peak of the clean Si(001)-(2×1) surface is attributed to disordered portion of the Si(001)-(2×1) surface.[9] By the adsorption of alkali atoms at the beginning, electron occupancy of these metallic states appears to be increased drastically. This is indicated by the initial increase of the peak. The slight shift of the peak can be understood if the density of states of the metallic states have a sharp maximum.

Upon further adsorption of alkali metals, the intensities of the metallic peaks decrease without changing the rest of the spectral features. This indicates that the dangling bond states in the area of disordered array of asymmetric dimers are filled by alkali valence electrons at first, then the filling of the dangling bond states itself changes the asymmetric dimers into symmetric ones to heal off the disorder. Indeed, LEED patterns at this stage of adsorption are clearer than those for clean Si(001)-(2×1) surfaces. For further alkali adsorption, the spectra change to those of the full-coverage Si(001)-(2×1)/K and Si(001)-(2×1)/Cs surfaces which are discussed in the following section.

TABLE I. Values of work function change for the K/Si(001) and Cs/Si(001) systems in eV. $\Delta\Phi_{max}$ is the change at maximum decrease and $\Delta\Phi_{sat}$ is the change at alkali saturation.

	K/Si(001) $\Delta\Phi_{max}$	$\Delta\Phi_{sat}$		Cs/Si(001) $\Delta\Phi_{max}$	$\Delta\Phi_{sat}$
Present	−3.33	−3.21	Present	−3.56	−3.11
Ref. 10[a]	−3.0	−2.6	Ref. 1	−3.8	−3.6
Ref. 12		~−2.0	Ref. 5	−3.7	−3.2
Ref. 8[b]	−3.6		Ref. 11	−3.4	−2.8

[a]On 200 K substrate.
[b]Only a single value is reported.

C. Coverage of alkali metals

As found in Sec. III, the full-coverage and intrinsic Si(001)-(2×1)/K and Si(001)-(2×1)/Cs surfaces are semiconducting. It is further said rather safely from this that the alkali coverage for the intrinsic Si(001)-(2×1)/K and Si(001)-(2×1)/Cs surfaces is 1 ML instead of $\frac{1}{2}$ ML as generally assumed. This statement is based on the following argument. Namely, if we have $\frac{1}{2}$ ML of K or Cs, the number of valence electrons available for surface states becomes odd per 2×1 unit cell. For example, the number of electrons of dangling bonds is 2, and the number of electrons of alkali atom is one. Therefore, the surface must be metallic in this case. If we have 1 ML of alkali atom, the number of valence electrons available for surface states becomes even, thus the surface can be semiconducting.

In a recent x-ray photoelectron-diffraction study, Abukawa and Kono[13] determined part of the geometry of the Si(001)-(2×1)/K surface. Their structural model is depicted in Fig. 12. There are two types of K sites, and the K coverage is indeed 1 ML.

D. Surface-state dispersions

Surface-state dispersions for the Si(001)-(2×1)/K and Si(001)-(2×1)/Cs surfaces are not obvious in Figs. 5 and 11. However, if we assume that the substrate Si dimers are intact for the Si(001)-(2×1)/K and Si(001)-(2×1)/Cs surfaces, hypothetical surface-state dispersions can be extracted from our results as shown in Fig. 13. For the clean Si(001)-(2×1) surface, dispersion of dimer dangling bond states is already known.[14] With this knowledge, the surface-state dispersion of a clean 2×1 surface in our experiment is drawn. The nature of the two-domain 2×1 surface is taken into account. When the substrate surface is covered with K or Cs as in Fig. 12, each of the dangling bond surface states must be provided by one electron from alkali atoms. Then the S_1 and S_2 bands of clean 2×1 surface may be doubled and may split for certain symmetry points for the alkali-adsorbed surfaces. Under this assumption, surface-state dispersions for the Si(001)-(2×1)/K and Si(001)-(2×1)/Cs surfaces are drawn in Fig. 13. For the Si(001)-(2×1)/K surface each of the S_1 and S_2 bands must have two components. This double component may be degenerated or the splitting is too small to be seen in ARUPS spectra. In fact, peaks for the S_2 band are broad in Fig. 4 indicating it is actually split. For the Si(001)-(2×1)/Cs surface, the otherwise S_2 band is actually split into the S_2 and S_3 bands. An unoccupied surface state as observed by inverse photoemission[8] may be ascribed to an antibonding state between the alkali s state and Si dangling bond state for the semiconductive Si(001)-(2×1)/K surface.

E. K 3p and Cs 5p core-level spectra

A surprising finding in Figs. 3 and 9 is that the energies of the core levels do not change in spite of the large change in work function. If charge transfer from alkali

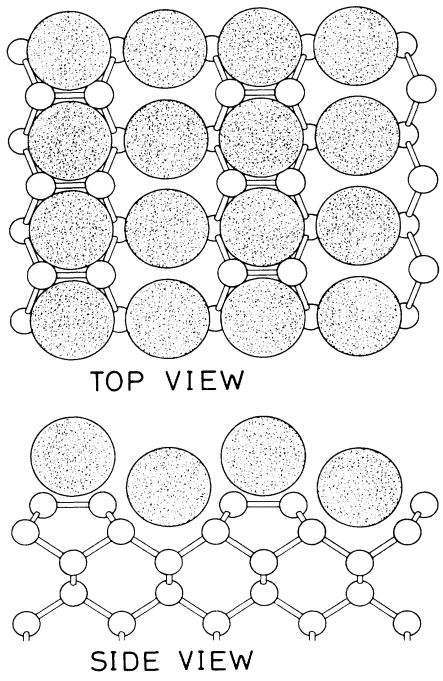

FIG. 12. Schematic illustration of Si(001)-(2×1)/K surface as proposed from x-ray photoelectron diffraction (Ref. 13). In the XPD study, only the geometry of K layers (shaded large circles) are determined and the relation to the Si dimers is an assumption.

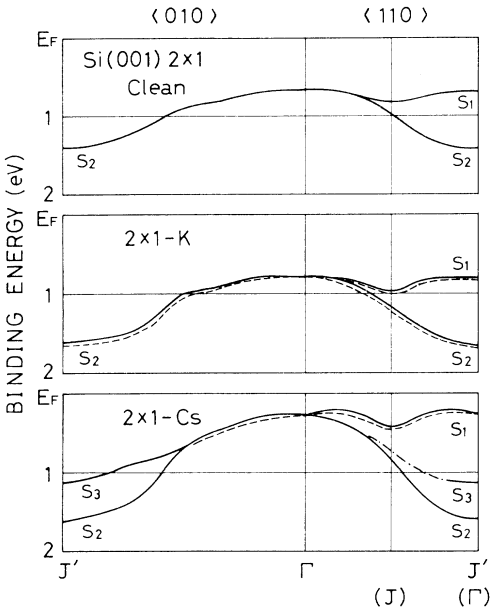

FIG. 13. Surface-state dispersions for the clean Si(001)-(2×1), Si(001)-(2×1)/K, and Si(001)-(2×1)/Cs surfaces as deduced from Figs. 5 and 11. It is assumed that the Si dimers are intact for the Si(001)-(2×1)/K and Si(001)-(2×1)/Cs surfaces. The two-domain 2×1 overlap is included. Dashed lines are bands that may be degenerated or splitted very little from the solid-line bands.

atom to the substrate is large, as generally assumed, the dipole field between the ionized alkali atoms and the substrate would increase resulting in a shift to higher binding energy of the alkali core electrons. Since this shift is not observed, the so-called charge transfer may not occur on these K/Si(001) and Cs/Si(001) systems. Recently, Ishida and Terakura[15] reported a first-principles calculation of electronic structure of Na/Al(001) surface. They found that the classical point-charge-transfer type of bonding is incorrect but the adatom-substrate bond has strong covalency.[15] The mechanism that causes work-function change is charge redistribution around alkali atoms, and the net charge of the alkali atom is not changed essentially.[15] If this type of covalent bonding is the case for K/Si(001) and Cs/Si(001) systems, there will not be much change in net potential around the alkali-atom site, which gives explanation to the present finding in the core-level spectra.

However, as discussed in Sec. V D the deduced surface-state dispersion, if it is correct, seems to be consistent with the view that the *s*-electron charge of alkali atoms transfers to the otherwise dangling bond of Si dimers. The invariance of the core-level position may need careful examination with theoretical analysis of the alkali-substrate bonding in the initial state of photoexcitation together with the theoretical analysis of screening of core hole in the final state of photoexcitation.

The Cs 5*p* spectra in Fig. 9 show broadening of the peaks. This may be due to the fact that there are two types of alkali-atom site, such as in Fig. 12, for the Cs/Si(001) system. Other causes of the change in spectral profile such as plasmon excitation and band formation may be involved in the core-level spectra for high coverage of K and Cs.

F. Effect of substrate doping

The effect of substrate doping appeared in the strength of the metallic peak for the clean Si(001)-(2×1) surface and for the alkali/Si(001) surfaces at early stage of alkali adsorption. The metallic peak is stronger for the high-dope *n*-type sample than for the nearly intrinsic sample. This may be understood by the population change in the E_F pinning surface state which may be controlled by bulk doping.[16] However, effect of substrate doping was not visible in the spectra of the semiconducting Si(001)-(2×1)/K and Si(001)-(2×1)/Cs surfaces; spectral positions and dispersions of the peaks are identical for the two kinds of substrates (results not shown). For a semiconducting surface, the E_F level at the surface would align to the E_F level of subsurface region of the substrate. The presence of *p*-type subsurface layer irrespective of bulk doping has been reported.[17] If we have this type of *p*-type subsurface layer in our substrate, the invariance of the ARUPS spectra for the semiconducting Si(001)-(2×1)/K and Si(001)-(2×1)/Cs surfaces can be understood. If this is the case, the doping dependence of the metallic-peak intensity for the clean and the lightly alkali-metal-adsorbed Si(001)-(2×1) surfaces must be related to the degree of surface order which may be affected by doping. Further study is needed to clarify these points.

V. CONCLUSIONS

Angle-resolved UPS spectra of valence bands and outermost *p* core levels of alkali-metal-element for the K/Si(001) and Cs/Si(001) systems have been measured. Full-coverage Si(001)-(2×1)/K and Si(001)-(2×1)/Cs surfaces are found to be semiconducting in contrast to a generally assumed one-dimensional alkali-metal chain structure for these surfaces. Plausible dispersions of surface states for the full-coverage (2×1)/K and (2×1)/Cs surfaces are deduced. It is supposed in the deduction that the Si dimer structure is intact even with full coverage of alkali metal and further assumed that the electronic states of the otherwise Si dimer dangling bonds are occupied by the *s* electrons of alkali metals. However, it is noted from the observation of alkali outermost core-level spectra that the bonding between the alkali-metal adatoms and the Si dimers may not be a charge-transfer type but is a covalent type.

Note added in proof. In a recent ARUPS study on a single-domain Si(001)-(2×1)/K surface, surface-state

disperions are determined.[18] Results showed two bands: one disperses around $\sim 0.8 < E_b < \sim 0.9$ eV along the $\bar{\Gamma}$-$\bar{J}$ direction and $\sim 0.8 < E_b < \sim 1.4$ eV along $\bar{\Gamma}$-$\bar{J}'$; the other $\sim 1.1 < E_b < \sim 1.6$ eV along $\bar{\Gamma}$-$\bar{J}$ and $\sim 1.3 < E_b < \sim 1.6$ eV along $\bar{\Gamma}$-$\bar{J}'$ directions. These bands appeared to be different than the deduced bands in Fig. 13.

ACKNOWLEDGMENT

The authors are grateful to Professor K. Terakura for letting us know his result prior to publication and for pointing us toward the possible cause of invariance in the core-level binding energies of alkali adatoms.

[1]R. Holtom and P. M. Gundry, Surf. Sci. **63**, 263 (1977).

[2]T. Aruga, H. Tochihara, and Y. Murata, Phys. Rev. Lett. **53**, 372 (1984).

[3]M. Tsukada, H. Ishida, and N. Shima, Phys. Rev. Lett. **53**, 376 (1984); H. Ishida, N. Shima, and M. Tsukada, Phys. Rev. B **32**, 6246 (1985).

[4]S. Ciraci and I. P. Batra, Phys. Rev. Lett. **56**, 877 (1986); Phys. Rev. B **37**, 2955 (1988).

[5]H. Tochihara and Y. Murata, J. Phys. Soc. Jpn. **51**, 2920 (1982).

[6]J. E. Ortega, E. M. Oellig, J. Ferrón, and R. Miranda, Phys. Rev. B **36**, 6213 (1987).

[7]Y. Enta, T. Kinoshita, S. Suzuki, and S. Kono, Phys. Rev. B **36**, 9801 (1987).

[8]I. P. Batra, J. M. Nicholls, and B. Reihl, J. Vac. Sci. Technol. A **5**, 898 (1987).

[9]Source of the metallic peak was examined for a Ge(001)-(2×1) surface; S. D. Kevan and N. G. Stoffel, Phys. Rev. Lett. **53**, 702 (1984); S. D. Kevan, Phys. Rev. B **32**, 2344 (1985).

[10]E. M. Oellig and R. Mirand, Surf. Sci. **177**, L947 (1986).

[11]J. E. Ortega, E. G. Oellig, J. Ferrón, and R. Mirand, Phys. Rev. B **36**, 6213 (1987).

[12]H. Tochihara, Surf. Sci. **126**, 523 (1983).

[13]T. Abukawa and S. Kono, Phys. Rev. B **37**, 9097 (1988).

[14]R. D. Bringans, R. I. G. Uhrberg, M. A. Olmstead, and R. Z. Bachrach, Phys. Rev. B **34**, 7447 (1986).

[15]H. Ishida and K. Terakura (unpublished).

[16]P. Martensson, A. Cricenti, and G. V. Hansson, Phys. Rev. B **33**, 8855 (1986).

[17]M. Liehr, M. Renier, R. A. Wachnik, and G. S. Scilla, J. Appl. Phys. **61**, 4619 (1987).

[18]Y. Enta, S. Suzuki, S. Kono, and T. Sakamoto (unpublished).